Quantification of electrogenerated chemiluminescence from tris(bipyridine)ruthenium(ii) and hydroxyl ions

Quantification of electrogenerated chemiluminescence from tris(bipyridine)ruthenium(II) and hydroxyl ions†

Andrea Fiorani, [a] Giovanni Valenti, [b] Irkham, [a] Francesco Paolucci[b] and Yasuaki Einaga *[a]

In this work, we quantify the electrogenerated chemiluminescence arising from the reaction of electro- generated tris(bipyridine)ruthenium(III) with hydroxyl ions, in terms of emission intensity and reaction rate. Different electrode materials (glassy carbon and boron-doped diamond) and different supporting electrolytes (perchlorate, phosphate, and carbonate) were investigated with pH variation. Relative quantification of the electrogenerated chemiluminescence was achieved using the $Ru(bpy)_3^{2+}$/tri-n- propylamine system, taken as a reference, with relative emission as low as 600 and 230 times that observed at the same coreactant concentration and the same pH, respectively. The kinetics was investigated by foot of the wave analysis of cyclic voltammetry to measure the turnover frequency of the reaction.

Introduction

The luminescent reaction of tris(bipyridine)ruthenium(III), abbreviated here Ru(III), with hydroxyl ions was first reported by Hercules and Lytle in 1966.[1] The chemical reduction of Ru(III) leads to the formation of a metal-to-ligand charge transfer (^{3}MLCT) triplet excited state,[2] which emits at around 610 nm.[3,4] Not only hydroxyl ions, but many molecules react with Ru(III) to give luminescence, making this reaction a power- ful tool for analytical applications,[5,6] and detecting amines,[7] amino acids,[8] and heteroaromatic compounds.[9] If Ru(III) is generated electrochemically from $Ru(bpy)_3^{2+}$, abbreviated here as Ru(II), this procedure as a whole is now an electrogenerated chemiluminescence (ECL) reaction, since it comprises an elec- trochemical step that triggers the light emission.[10–12] Examples of this application include the detection of ascorbic and dehydroas- corbic acids,[13] oxalate, ethanol and sulfite,[14] formaldehyde and formic acid,[15] thiocholine,[16] hydrazine,[17] methamphetamine,[18] and sarcosine,[19] a prostate cancer marker. In the mentioned examples, Ru(II) is free to diffuse in solution and the molecules detected by ECL can also act as coreactants, since they can be oxidized at the electrode, resembling the usual ECL system of Ru(II) and tri-n-propylamine (TPrA).[20] Since all these applications are conducted in water solution, the luminescence reaction of Ru(III) with hydroxyl ions should be observed to some extent, and it might generate a detectable background signal that cannot be neglected. Many ECL research papers[21] refer to this chemiluminescence reaction described by Hercules and Lytle to justify the background emission concurrent to the oxidation of Ru(II) in aqueous solutions. Instead, we present a measure of this light emission directly by ECL. Here, we investigated the reaction kinetics and the effect of pH on the reaction of Ru(III) with hydroxyl ions through the ECL of Ru(II) in water solution, by comparing different electrolytes and electrode materials. The relative ECL emission was quantified against the well- known Ru(II)/TPrA system. We must recall that hydroxyl ions do not react at the electrode to give the ECL reaction, only Ru(II) is oxidized, following eqn (1) and (2), similar to the catalytic mechanism of Ru(II)/TPrA.[22]

$Ru(bpy)^{2+}$ e - $Ru(bpy)^{3+}$ (1) 33

$Ru(bpy)_3^{3+} + OH$ - $Ru(bpy)_3^{2+}* +$ products (2)

The reaction mechanism described by eqn (1) and (2) might be an oversimplification of the real mechanism leading to light emission, however it is justified in order to rationalise the kinetics of the bimolecular reaction between Ru(III) and OH (see ESI,† Parts 1 and 2).

Experimental

$Ru(bpy)_3Cl_2 6H_2O$, $NaClO_4$, Na_3PO_4, Na_2SO_4, Na_2CO_3, H_3PO_4, $HClO_4$ and NaOH were purchased from Wako Pure Chemical (JP),

and TPrA was purchased from Sigma Aldrich (USA), and they were used without further purification. All solutions were prepared in pure double distilled water (ddw) with a resistivity of 18 MO cm, from a SimplyLab water system (DIRECT-Q3 UV, Millipore). Before each measurement, the GC (Tokai Carbon, JP) electrode was cleaned with a 0.5 mm alumina powder suspension on cloth tape, then sonicated in ddw for 5 min, rinsed in ddw, and dried in a nitrogen stream. BDD fabrication and

ECL instrumentation were explained in detail in ref. 23. The BDD electrode (1% B/C) was cleaned by sonication in isopropanol for 5 min, rinsed in ddw, and dried in a nitrogen stream. Prior to each measurement, the BDD surface was pretreated electrochemically, by performing 10 voltammetric cycles between 2.0 and 2.0 V followed by 10 cycles between 0 and 2.0 V in a 0.1 M $NaClO_4$ solution at a scan rate of 0.3 V s^1. All potentials throughout the text are referenced to the Ag/AgCl (saturated KCl) electrode. ECL spectra were collected using a SEC2000 Spectra system UV-visible spectrophotometer (ALS Co., JP). NaOH was used to adjust the pH of the $NaClO_4$ solution, $HClO_4$ was used to adjust the pH of the Na_2CO_3 solution and H_3PO_4 was used to adjust the pH of the Na_3PO_4 solution. All measurements were performed in triplicate.

Results and discussion

The ECL of Ru(II) arising from cyclic voltammetry with a glassy carbon (GC) electrode in perchlorate and phosphate electrolytes is shown in Fig. 1.

In both electrolytes, ECL starts at the oxidation potential of Ru(II) ($E_{1/2}$ = 1.07 V, see ESI†), confirming the participation of Ru(III) in the mechanism, with two peaks around 1.1 and 1.4 V.

The effect of pH was investigated by changing the pH of the pure phosphate solution to pH 5 by the addition of acid. Perchlorate solution was added with hydroxide, to change the solution pH from pH 5 to 13.

ECL emission as a function of pH is reported in Fig. 2 and Fig. S1 (ESI†). Perchlorate and phosphate addition results in the same trend of ECL for the first peak, while a clear effect of the buffer capacity of phosphate is evident in the second peak, with a shift of ECL emission at a lower pH of 0.8 units (Fig. 2 and Fig. S1, ESI†). The double peak shape is very reproducible, and furthermore it seems to depend on the relative Ru(II)/OH ratio (Fig. S3, ESI†). For phosphate, a detectable ECL emission (i.e., higher that the measurement noise) is clear from pH 7, a usual value in ECL measurements, which can contribute to background ECL. Carbonate has also been used as an electrolyte, however it can be oxidized in the same potential range of ECL emission, which impairs the correct measurement of the light intensity (Fig. S2, ESI†). Comparison of the obtained ECL with that of the most used Ru(II)/TPrA system gives a relative quantification of the emis- sion (Fig. S3, ESI†). Very similar ECL signals are measured for largely different concentrations of luminophore and coreactant, 1 mM Ru(II)/ 1 M OH and 100 mM Ru(II)/100 mM TPrA (Fig. 3). At the same pH and Ru(II) concentration, the ECL from OH in phosphate buffer is about 230 times lower compared to that of Ru(II)/TPrA, which makes the Ru(II)/OH system unlikely to give any relevant contribution to the background emission at neutral pH.[24] Finally, we report the data from ECL quantification to high- light the finding of this investigation in Table 1. Furthermore, the TPrA concentration used in this case is lower than that commonly used for ECL study with Ru(II), on the order of hundreds of mM, which can make the contribution of Ru(II)/OH ECL even less relevant. An opposite result was observed when a boron doped diamond (BDD) electrode was used. BDD is a very well-known electrode material able to oxidize OH to OH.[25,26] The same experiments as those of Fig. 1 show no ECL emission in perchlorate and phosphate electrolytes (Fig. 4), while a detectable emission is measured for carbonate, although it is 5 times lower (Fig. S4, ESI†). In this case, we speculate that the depletion of OH in the diffusion layer is enough to quench the ECL emission. This evidence is also an indication that hydroxyl radical (OH) does not take part in the ECL reaction mechanism, since this is the main product of OH oxidation at the BDD electrode.

We ruled out the interference of the counter electrode and the effect of dissolved oxygen on ECL emission with dedicated experiments (Fig. S5, ESI†).

Finally, ECL spectral comparison of NaOH and TPrA core- actants permitted us to identify the emitting excited state (Fig. S6, ESI†). ECL is emitted from the ^{3}MLCT excited stated of Ru(II) with a peak centered around 610 nm, in line with the previous experiments of Ru(II) ECL.[23]

This confirms that both peaks lead to the generation of Ru(II)*, however the overall mechanism is still unclear (ESI,† Part 2). The fact that we cannot identify exactly the real step involved in the generation of the excited state makes it difficult for any prediction of the energetics and thus the efficiency of this reaction.

In order to describe the reaction kinetics, we tentatively investigated the reactivity of Ru(III) toward hydroxide by foot-of-the-wave analysis of cyclic voltammetry. This approach, devel- oped by Savéant and coworkers,[27–31] allows us to obtain the relationship between turnover frequency (TOF) and overpoten- tial (Z), as shown in the catalytic Tafel plot (Fig. 5, ESI,† Part 1). The reaction analyzed is depicted in Scheme 1; however, if it may involve several steps, they are equivalent to an overall reaction with an apparent rate constant k_{OH}.[27] Moreover, this approach is applicable and reliable when side-phenomena are encountered, (e.g., consumption of the substrate, deactivation of the catalyst, inhibition by products), which permits us to focus on the catalytic parameters, while discarding the side-effects.[27] This methodology was successfully tested on ruthenium

catalysts for water oxidation[32] and the results were found to be in agreement with constants derived spectroscopically,[33] which further validates this analysis. The CVs and their elaboration to obtain the TOF–Z plot are available in the ESI† (Fig. S7–S9).

The mechanism resembles water nucleophilic attack (WNA), in analogy to ruthenium–oxo complexes for water oxidation, where the primary pathway involves a nucleophilic attack of an uncoordinated water molecule.[36–39] The TOF for the reaction given in Scheme 1 was measured for different concentrations of NaOH, and the results are shown in Fig. 5 and Table 2.

Ru(II) results in very low TOF values. For the sake of comparison, we report the TOF values of a ruthenium–oxo complex[32] for water oxidation. The intrinsic turnover frequency (TOF_0), which is the TOF at zero overpotential and describes the intrinsic performance of the electrocatalyst, for Ru(II) is five orders of magnitude lower,[32,40] and reaching TOF_{MAX} requires a higher overpotential.

However, in this case, the TOF for Ru(II) does not represent the reaction kinetics of water oxidation, since O_2 formation is more the exception than the rule;[41] rather it provides informa- tion about the rate of the bimolecular reaction between Ru(III) and OH, which is similar to the WNA mechanism of ruthe- nium–oxo catalysts.

The results were compared with the catalytic constant (k_{obs}) of production of Ru(II) from the reduction of Ru(III) in alkaline solution (Fig. 6), as obtained by stopped-flow spectrophotome- try by Creutz and Sutin.[42]

Discrepancies may arise because the two techniques are different (spectroscopic or electrochemical);[33] moreover, the largest difference is obtained at a concentration out of the range of validity of the spectroscopic derived constant at 1 M hydroxide.

Conclusions

We presented a quantification of the reaction of electrogenerated tris(bipyridine)ruthenium(III) in aqueous alkaline solutions, in terms of ECL emission and reaction rate, which could be useful in the interpretation of results obtained using ECL in aqueous solution involving freely diffusing Ru(II). The ECL intensity is far below that the standard Ru(II)/TPrA system, i.e., 600 and 230 times at the same coreactant concentration and the same pH, respectively. The com- parison of different electrolytes and electrode materials shows the effect of buffer capacity and hydroxyl ions on the ECL emission.

A description of the reaction rate by cyclic voltammetry analy- sis showed an extremely low intrinsic TOF_0 ($E10^{11}$–10^{13} s^1), while it reaches a maximum value at high overpotential, which is comparable with the kinetic constants derived from spectrophoto- metric measurements by Creutz and Sutin.

Conflicts of interest

There are no conflicts to declare.

Acknowledgements

This study was partially supported by JST-ACCEL and a Grant- in-Aid for Scientific Research A 19H00832 (to Y. E.). A. F. acknowledges the Japan Society for the Promotion of Science (Fellowship ID No. P19333) and KAKENHI Grant-in-Aid for JSPS Fellows (19F19333).

References

1 D. M. Hercules and F. E. Lytle, J. Am. Chem. Soc., 1966, 88, 4745.

2 S. Campagna, F. Puntoriero, F. Nastasi, G. Bergamini and V. Balzani, in Photochemistry and Photophysics of Coordina- tion Compounds I, ed. V. Balzani and S. Campagna, Springer- Verlag, Berlin, 2007, vol. 280, pp. 117–214.

3 N. E. Tokel and A. J. Bard, J. Am. Chem. Soc., 1972, 94, 2862. 4 F. E. Lytle and D. M. Hercules, J. Am. Chem. Soc., 1969, 91, 253.
5 G. P. McDermott, P. Jones, N. W. Barnett, D. N. Donaldson and P. S. Francis, Anal. Chem., 2011, 83, 5453.
6 R. D. Gerardi, N. W. Barnett and P. Jones, Anal. Chim. Acta, 1999, 388, 1.

7 J. B. Noffsinger and N. D. Danielson, Anal. Chem., 1987, 59, 865.
8 S. N. Brune and D. R. Bobbitt, Talanta, 1991, 38, 419–424. 9 H. Kodamatani, Y. Komatsu, S. Yamazaki and K. Saito, Anal. Sci., 2007, 23, 407.
10 A. Fiorani, G. Valenti, M. Iurlo, M. Marcaccio and F. Paolucci, Curr. Opin. Electrochem., 2018, 8, 31.

11 A. Zanut, A. Fiorani, S. Rebeccani, S. Kesarkar and G. Valenti, Anal. Bioanal. Chem., 2019, 411, 4375.

12 A. Fiorani, J. P. Merino, A. Zanut, A. Criado, G. Valenti, M. Prato and F. Paolucci, Curr. Opin. Electrochem., 2019, 16, 66.

13 M. Zorzi, P. Pastore and F. Magno, Anal. Chem., 2000, 72, 4934.

14 J.-M. Lin, F. Qu and M. Yamada, Anal. Bioanal. Chem., 2002,

374, 1159.

15 L. Hu, H. Li, S. Han and G. Xu, J. Electroanal. Chem., 2011,

656, 289.

16 R. Kurita, K. Arai, K. Nakamoto, D. Kato and O. Niwa, Anal.

Chem., 2010, 82, 1692.

17 L. Hu, J. Gao, Y. Wang and G. Xu, Anal. Methods, 2011, 3, 1786.

18 F. Takahashi, S. Nitta, R. Shimizu and J. Jin, Forensic Toxicol., 2018, 36, 185.

19 G. Valenti, E. Rampazzo, E. Biavardi, E. Villani, G. Fracasso, M. Marcaccio, F. Bertani, D. Ramarli, E. Dalcanale, F. Paolucci and L. Prodi, Faraday Discuss., 2015, 185, 299.

20 J. K. Leland and M. J. Powell, J. Electrochem. Soc., 1990, 137, 3127.

21 Out of 152 citations for ref. 1 and 54 are from ECL papers (SCOPUS, March 2020).

22 W. Miao, J.-P. Choi and A. J. Bard, J. Am. Chem. Soc., 2002, 124, 14478.

23 A. Fiorani, Irkham, G. Valenti, F. Paolucci and Y. Einaga, Anal. Chem., 2018, 90, 12959.

24 S. Carrara, F. Arcudi, M. Prato and L. De Cola, Angew. Chem., Int. Ed., 2017, 56, 4757.

25 N. Yang, S. Yu, J. V. Macpherson, Y. Einaga, H. Zhao, G. Zhao, G. M. Swain and X. Jiang, Chem. Soc. Rev., 2019,

48, 157.

26 Irkham, T. Watanabe and Y. Einaga, Anal. Chem., 2017, 89, 7139.

27 I. Bhugun, D. Lexa and J.-M. Sav´eant, J. Am. Chem. Soc., 1996, 118, 1769.

28 C. Costentin, S. Drouet, M. Robert and J.-M. Sav´eant, J. Am. Chem. Soc., 2012, 134, 11235.

29 C. Costentin and J.-M. Sav´eant, ChemElectroChem, 2014, 1, 1226. 30 C. Costentin, G. Passard and J.-M. Sav´eant, J. Am. Chem. Soc., 2015, 137, 5461.
31 C.CostentinandJ.-M.Sav´eant,J.Am.Chem.Soc.,2017, 139, 8245.
32 R. Matheu, S. Neudeck, F. Meyer, X. Sala and A. Llobet, ChemSusChem, 2016, 9, 3361.
33 D. J. Wasylenko, C. Rodr´ıguez, M. L. Pegis and J. M. Mayer, J. Am. Chem. Soc., 2014, 136, 12544.

34 C. R. Martin, I. Rubinstein and A. J. Bard, J. Electroanal. Chem., 1983, 151, 267.
35 P. Dongare, B. D. B. Myron, L. Wang, D. W. Thompson and T. J. Meyer, Coord. Chem. Rev., 2017, 345, 86.
36 X.Sala,S.Maji,R.Bofill,J.Garc´ıa-Ant´on,L.Escricheand A. Llobet, Acc. Chem. Res., 2014, 47, 504.
37 J. D. Blakemore, R. H. Crabtree and G. W. Brudvig, Chem. Rev., 2015, 115, 12974.
38 D. W. Shaffer, Y. Xie and J. J. Concepcion, Chem. Soc. Rev., 2017, 46, 6170.
39 Z. N. Zahran, Y. Tsubonouchi, E. A. Mohamed and M. Yagi, ChemSusChem, 2019, 12, 1775.
40 R. Matheu, M. Z. Ertem, J. Benet-Buchholz, E. Coronado, V. S. Batista, X. Sala and A. Llobet, J. Am. Chem. Soc., 2015, 137, 10786.
41 P. K. Ghosh, B. S. Brunschwig, M. Chou, C. Creutz and N. Sutin, J. Am. Chem. Soc., 1984, 106, 4772.
42 C. Creutz and N. Sutin, Proc. Natl. Acad. Sci., U. S. A., 1975, 72, 2858.

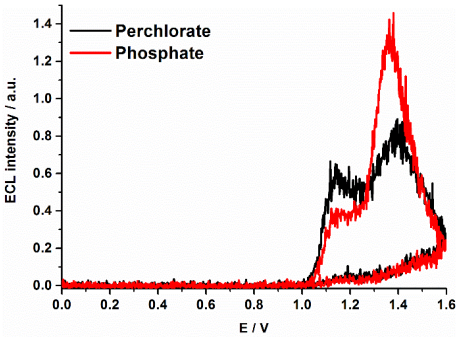

Fig. 1 ECL intensity of 100 □M Ru(II) in different electrolytes at GC electrode: perchlorate (black) pH 13 and phosphate (red) pH 12.5, solutions 100 mM each. Scan rate 100 mVs-1.

Fig. 2 ECL emission intensity at different pH, from cyclic voltammetry with scan rate 100 mVs-1: perchlorate (black) and phosphate (red) 100 mM solutions; first peak at 1.1 V (empty symbols) and second peak at 1.4 V (filled symbols). Ru(II) is 100 □M. Lines are drawn only as guides for the eye.

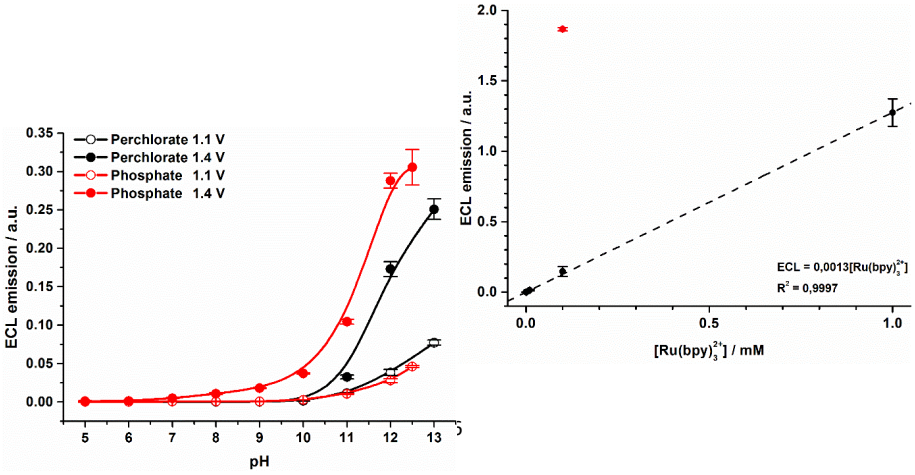

Fig. 3 Calibration of Ru(II) in 1 M NaOH, integrated ECL signal from 0 V to 1.6 V; the red point is from 100 μM Ru(II) and 100 μM TPrA in 0.2 M phosphate buffer at pH 7.5 (Fig. S3).

Table 1. Comparison of Ru(II)/TPrA and Ru(II)/OH^- ECL emission. [a]Same [TPrA] and [OH^-]. [b]Same pH and electrolyte (PO_4^{3-}).

	ECL	Ratio
[TPrA] / 100 μM	1.87 ± 0.01	
ClO_4^- / pH 10[a]	0.0031 ± 0.0004	600 ± 80
PO_4^{3-} / pH 7.4[b]	0.0080 ± 0.0010	230 ± 30

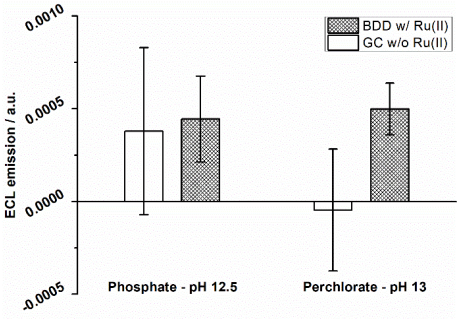

Fig. 4 Integrated ECL signal from CV-ECL, GC without and BDD with 100 μM Ru(II) in 100 mM supporting electrolyte at the specified pH.

$$\rightarrow Ru(bpy)_3^{2+} \overset{E_{1/2},\, k^0}{\rightleftharpoons} Ru(bpy)_3^{3+} + e^-$$

$$Ru(bpy)_3^{3+} + OH^- \xrightarrow{k_{OH}} Ru(bpy)_3^{2+*} + \text{products}$$

$$Ru(bpy)_3^{2+*} \xrightarrow{k_{ph}} Ru(bpy)_3^{2+} + h\nu$$

Scheme 1 Model of the catalytic reaction based on one-electron/one-step process,[28] **Errore. Il segnalibro non è definito.** to be applied for foot-of-the-wave analysis. $E_{1/2}$ is the half-wave potential of the couple $Ru^{3+/2+}$ = 1.07 V, and k^0 is the

heterogeneous electron transfer constant (0.06 cm s^{-1}).[32] k_{OH} is the apparent catalytic rate constant. k_{ph} is the rate constant for phosphorescence decay (6.5×10^4 s^{-1}).[33]

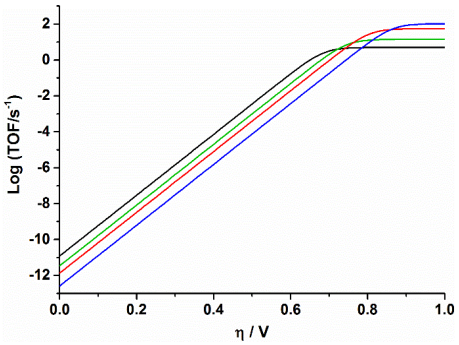

Fig. 5 Catalytic Tafel plot of Ru(II) in NaOH 1 (black), 10 (green), 100 (red), and 1000 (blue) mM with in Na_2SO_4 100 mM.

Table 2 Values of TOF from Figure 5. a) Ruthenium-oxo complex at pH 7, from ref. 30.

OH^- / M	1	0.1	0.01	0.001	$^aRu^{IV}$
TOF_{MAX} / s^{-1}	105	55	14	5	7700
Log (TOF_0 / s^-	-12.5	-11.9	-11.5	-10.9	-6.5

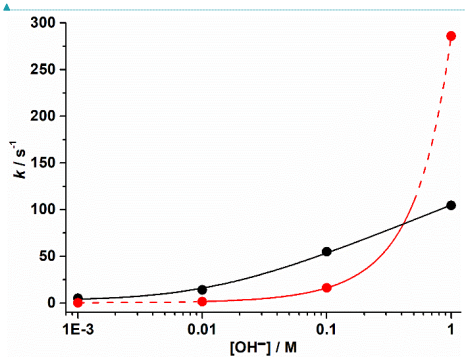

Fig. 6 Catalytic constants (k): Ru(II) production from the reduction of Ru(III) by hydroxyl ions within the range of validity (red line, full), and beyond the range of validity (red line, dashed), adapted from ref. 40 (kobs/s-1); TOFMAX/s-1 (black dots), line is only as guide for the eye.

Formattato: Tipo di carattere: (Predefinito) Times New Roman, Grassetto, Colore carattere: Testo 1